Arch. Metall. Mater., Vol. 61 (2016), No 4, p. 2091–2096

DOI: 10.1515/amm-2016-0336

D. KALISZ*#, P.L. ŻAK*, K. KUGLIN*

# ANALYSIS OF AGGLOMERATION OF $Al_2O_3$ PARTICLES IN LIQUID STEEL

The removal of non-metallic inclusions from liquid steel is a result of co-operation of fluctuation, adhesion and agglomeration effects, with emphasis on agglomeration which plays the most important role. It is based on a few types of collisions between non-metallic particles, where turbulent collisions are most prominent. As a result of agglomeration, non-metallic inclusions are intensely removed through flotation and increase of different dimensions of inclusions, which manifests itself with the occurrence of clusters mainly composed of $Al_2O_3$ precipitations. Authors investigated the agglomeration effect by making computer simulations with the use of the PSG method. The calculations were performed for a definite population of spherical particles of radius *r* in the steel volume. The applied calculation method allows for analyzing the dynamics of the collision process. The assumed initial number of particles remains constant, only the number of particles in specific size-groups varies. It was also revealed that the process of agglomerates formation is much faster for particles having a bigger initial radius. In the case of very small precipitations (r=1 μm) their removal through agglomeration is very difficult because the probability those collisions can take place between them rapidly decreases.

*Keywords*: steel, agglomeration, non-metallic inclusion, PSG Method

## 1. Introduction

The technology of steel production covers such elements as generation, growth and removal of non-metallic precipitates. The products of deoxidization are the main contaminants of liquid steel therefore the removal of primary non-metallic inclusions is a key task of refining. The production of a given quantity of secondary inclusions of desired chemical composition and size is a consequence of processes taking place in the CCS (Continuous Casting of Steel) crystallizer. The final result of this phenomenon is the controlled distribution of inclusions in a given ingot.

The experiments on the behavior of non-metallic inclusions in liquid steel performed by authors [1-5] show that non-metallic particles are not uniformly liable to agglomeration. Three groups of precipitates could be distinguished on the basis of the analysis of morphology of non-metallic inclusions [6]:

- solid: e.g. $Al_2O_3$, 80% $Al_2O_3$-CaO, $Al_2O_3$-CaO-95%$SiO_2$,
- liquid: e.g. 50%$Al_2O_3$-40%CaO-MgO, $Al_2O_3$-MnO-$SiO_2$, 60% $Al_2O_3$-CaO-$SiO_2$,
- Complex: (solid core in liquid cover), e.g. 60%$Al_2O_3$-32%CaO-MgO.

In the case of solid non-metallic inclusions, e.g. pure $Al_2O_3$ precipitates or with a small addition of CaO or $SiO_2$, their shape is irregular and far from spherical. More regular are precipitates with $SiO_2$ content the complex liquid or semi liquid precipitates are deformed when flowing out of liquid steel, and assuming a lens shape on its surface. The physical form and chemical composition of non-metallic inclusions determine the way in which the particles attract themselves. Another important effect is the adhesion and wettability of a given non-metallic phase by liquid metal.

Experiments on the behavior of inclusions on the liquid steel/noble gas interface conducted by H. Yin et al. [1-2] proved that solid CaO-$Al_2O_3$ precipitates and solid CaO-$Al_2O_3$-$SiO_2$ inclusions agglomerate faster, forming clusters and then undergoing deformation. Small particles move towards the larger, almost immobile ones. Colliding particles make the inclusions form groups, then clusters and larger aggregates. Authors proved that capillary attraction is responsible for this mechanism. Solid particles of similar chemical composition act on themselves to the greatest extent. Attraction between a solid and liquid or semi liquid particle is much smaller. If such precipitates are involved, physicochemical phenomena accompanying the contact of particles of different state should be simultaneously considered. These are processes responsible for mutual dissolving of phases and possible chemical reaction taking place in the precipitates area. As a result new precipitates are formed, being a consequence of reactions and phase transformations. The new phases differ from the source material with shape, state and melting temperature. If a solid particle is bigger than its liquid counterpart, it will be covered by it, otherwise it will be absorbed by the bigger one and the new precipitation will be spherical in shape.

Yin et al. [1-2] have observed a strong attraction between alumina and particles mainly composed of $Al_2O_3$. It was also noted that the attraction over 10-16 N acts on particles more than 3μm in size within an area exceeding 10μm. This means that alumina precipitates or predominantly composed of it; show a broader range of impact, facilitating their easy agglomeration. The particles are entrained if the angle of

* AGH UNIVERSITY OF SCIENCE AND TECHNOLOGY, FACULTY OF FOUNDRY ENGINEERING, AL. A. MICKIEWICZA 30, 30-059 KRAKÓW, POLAND

# Correspondin author: dak@agh.edu.pl

wettability of both inclusions is smaller or bigger than $90^0$.

Based on the angle of wettability, authors [1-2] classified the oxides as: $BeO>Al_2O_3(135^0)>SiO_2>ZrO_2>CaO>MgO\sim90^0$. This classification corresponds to the decreasing agglomeration ability of specific particles. It was also observed that the force of attraction does not depend on the composition of the metal bath. The formation of $Al_2O_3$ clusters affects the rate of precipitates removal by their flowing out from the liquid steel. If a large cluster of $Al_2O_3$ particles does not manage to flow out or adhere to the ceramic surface, it is a material defect of steel.

## 2. Agglomeration mechanism

The mechanism of inclusions removal is based on the process of fluctuation, adhesion and agglomeration. Agglomeration can refer to solid particles – coagulation of liquid particles – to coalescence. Non-metallic inclusions are formed as a result of nucleation, and then they grow and collide with other particles, resulting in the formation of bigger inclusions. The most important role is played by collision-based agglomeration. The frequency of collision between particles "*i*" and "*j*" is given by the formula [3,7-8]:

$$N_{ij} = \beta(V_i, V_j) \cdot n_i \cdot n_j \tag{1}$$

where:
$N_{i,j}$ – number of collisions between two types of particles per unit of time and unit of volume,
$V_i$, $V_j$ – volume of particles,
$\beta(V_i,V_j)$ – function defining frequency of collisions of their given type, for a definite volume of particles ($m^3/s$),
$n_i$, $n_j$ – concentration of particles "i" and "j" ($m^{-3}$).

The particles may form aggregates in liquid steel as a result of collisions:

- due to Brownian motion,

$$\beta_B(\mathrm{V}_i, \mathrm{V}_j) = \frac{2 \cdot k \cdot T}{3 \cdot \mu} \cdot \left(\frac{1}{r_i^{1/3}} + \frac{1}{r_j^{1/3}}\right) \cdot \left(r_i^{1/3} + r_j^{1/3}\right) \tag{2}$$

where:
$k$ – Boltzman constant (J/K),
$\mu$ - viscosity of liquid metal (Pa·s).

- Due to differences in the rate of their flowing out,

$$\beta_S(\mathrm{V}_i, \mathrm{V}_j) = \pi \cdot \left(r_i - r_j\right)^2 \cdot \left(r_i - r_j\right) \tag{3}$$

- Turbulent collisions,

$$\beta_T(\mathrm{V}_i, \mathrm{V}_j) = 1.3 \cdot \alpha_T \cdot \left(r_i + r_j\right)^3 \cdot \left(\frac{\varepsilon}{\nu}\right)^{1/2} \tag{4}$$

where:
$r_i$, $r_j$ – radii of particles,
$\varepsilon$ – rate of dispersion of turbulent kinetic energy ($m^2/s^3$),
$\nu$ – kinematic viscosity of metal ($m^2/s$),
$\alpha_T$ – coefficient of coagulation.

Three types of collisions may occur simultaneously. Then the frequency coefficient is a sum of particular types [9]:

$$\beta(r_i, r_j) = \beta_B(r_i, r_j) + \beta_T(r_i, r_j) + \beta_S(r_i, r_j) \tag{5}$$

$$\beta(r_i, r_j) = \left[\frac{2 \cdot k \cdot T}{3 \cdot \mu} \cdot \left(\frac{1}{r_i^{\frac{1}{3}}} + \frac{1}{r_j^{\frac{1}{3}}}\right) \cdot \left(r + r_j^{\frac{1}{3}}\right)\right] + \left[1.3 \cdot \alpha_T \cdot \left(r_i + r_j\right)^3 \cdot \left(\frac{\varepsilon}{\nu}\right)^{\frac{1}{2}}\right] + \left[\pi \cdot \left(r_i - r_j\right)^2 \cdot \left(r_i - r_j\right)\right] \tag{6}$$

The efficiency of collisions as a result of Brownian motion is very low. The Stokes mechanism of collision and turbulent collision have similar values of constant rates at low mixing capacity. For metallurgical processes taking place in the ladle during refining and casting the mixing is a very powerful process making the turbulent collisions plays a dominating role. The analysis of agglomeration of non-metallic particles due to collision in a specific volume of liquid phase created many problems. The Particle Size Grouping (PSG) is one of the methods thanks to which the analysis of the interaction of the particles is much easier.

## 3. Calculation procedure

The agglomeration of precipitates in liquid steel causes not only their more intense removal by flotation, but also an increase of the number of large amounts of precipitates in the final product. The Particle Size Grouping (PSG) method allows for calculating an agglomeration for a small number of "size groups " of non-metallic inclusions, maintaining volume balance of precipitates. The PSG method was used in this paper for calculating agglomeration of $Al_2O_3$ inclusions in liquid steel. The analyzed population of particles has been described for the simplest case by the size of particles (radius r) and their number in a unit of steel volume, i.e. density n in the form of a figure. A full description, i.e. distribution of density of particles population requires a continuous function $n = f(r)$. Particles are connecting due to the operation of various mechanisms; therefore the distribution of density varies over the process duration. During agglomeration the non-metallic inclusions in liquid steel can be described with the use of numerical models. Saffman and Turner proposed a model of turbulent collisions, where during collisions of two different particles of radius ri and rj in liquid steel, part of the collisions $N_{ij}$ equals to [9-11]:

$$N_{ij} = 1.3\ (r_i + r_j)^3 \cdot (\varepsilon/\nu)^{1/2} n_i n_j \tag{7}$$

where:
$r$ – radius of particle,
$\varepsilon$– mixing energy [$m^2 \cdot s^{-3}$],
$\nu$ –kinematic viscosity of liquid [$m^2 \cdot s^{-1}$],
$n$ – density of particles,

Higashitani [11] accounted for agglomeration coefficient $\alpha$ in the collision frequency equation and the result of operation of viscosity forces in the course of liquid removal from between the colliding particles, and also van der Waals forces. Coefficient $\alpha$ in equation (8) depends on the radius of agglomeration.

$$N_{ij} = \alpha\,[1.3(r_i+r_j)^3\cdot(\varepsilon/v)^{1/2} n_i n_j] \tag{8}$$

The behavior of the system for particles built on the basis of previous collisions with k smallest particles is described with a population balance equation:

$$\frac{dn_k}{dt} = \frac{1}{2}\sum_{i=1,i+j=k}^{i=k-1}\left(1+\delta_{ij}\right)\cdot N_{ij} - \sum_{i=1}^{\infty}\left(1+\delta_{ik}\right)\cdot N_{ik} \tag{9}$$

$\delta_{ij}$ - delta Kronecker: $\delta_{ij} = 1$ for i = j and $\delta_{ij} = 0$ for i ≠ j,
$N_{ij}$ – number of collisions between particles *i* , *j* in 1 m$^3$ during one second,
$N_{ik}$ – number of collisions between particles i, k in 1 m$^3$ during one second.

Kronecker delta ($\delta_{ij}$) and ½ coefficient have been introduced to avoid double calculation of collisions of identical particles. If *k* denotes the number of smallest elements making up the analyzed particle, the first member of the population balance equation counts all collisions in the course of which k-particles of a given size are formed. A lot of possibilities of such collisions exist, e.g. (*k*-3) + (3), (*k*-2) + (2), etc. The first member on the right side of the equation sums up collisions, which caused a transition of smaller particles to class "*k*".

The second member counts all collisions in the course of which *k*-particles are liquidated; the collision of a *k*-particle with any other particle causes that the former stops being a *k*-particle. The solving of the population balance equation for *k* expressed by the successive natural numbers is a huge calculation task, therefore a simplified method making use of a small number of particle sizes was introduce. This leads to the grouping of many particles in one size class, and the population balance equation is solved only for these classes. By assuming a division of all particles into *M* classes we take into account only particles representative for a given class of volume from *v*1 to $v_M$. The ratio $v_k/v_{k-1} = R$ should be maintained constant. If we assume *R = 2*, then the critical particle *vk* is formed by two particles one level lower $v_{k-1}$. The assumed value of radius of spherical particles is rk and the successive threshold values of radius are $R_{k-1}$, $R_k$ and $R_{k+1}$; they decide about the class, to which a given particle belongs. In Nakaoka et al. [7] authors use dimensionless values. Dimensionless density denotes density $n_k$ referred to the density of the smallest particles making up the *N*0 system.

$$n_k^* = \frac{n_k}{N_0} \tag{10}$$

$$\frac{dn_k^*}{dt^*} = \sum_{i=i_{c,k-1}}^{k-1}\xi_{i,k-1}(r_1^* + r_{k-1}^*)^3 n_i^* n_{k-1}^* + \sum_{i=1}^{i_{c,k-1}}\zeta_{i,k}(r_i^* + r_k^*)^3\, n_i^* n_k^* - \sum_{i=i_{c,k}}^{M-1}(1+\delta_{ik})(r_i^* + r_k^*)^3 n_i^* n_k^* \tag{11}$$

where:
$n_i^* n_k^*$ – density of particles of given size is referred to the initial density of particles $N_0$,
$N_0$ – initial density of particles,
$N_M$ – number of particles forming a bigger agglomeration,
$\xi$, $\zeta$ – correction factors of particles density in a group,
$i_{c,k-1}$ – critical size of particles,

$$\xi_{i,k-1} = (vi + v_{k-1})/v_k \tag{12}$$

$$\zeta_{i,k} = v_i/v_k \tag{13}$$

$$r_k^* = r_k/r_1 \tag{14}$$

$$t^* = 1.3 \propto r_1^3(\varepsilon/v)^{1/2} N_0 t \tag{15}$$

t* - dimensionless time

The right side of equation (11):

- Participation of collisions in which particles "*k*-1" are formed with particles "*k*"
- Participation of collisions with small particles, in which small particles "*k*" remain particles "*k*",
- Participation of collisions, in which particles "*k*" become bigger particles than "*k*".

The first member of the right side of equation (11) sums up the collisions. As a result smaller particles make a transition to class "*k*" (16).

$$\sum_{i(kryt)_k}^{k-1}\xi_{i,k-1}\cdot\left(r_i^* + r_{k-1}^*\right)^3\cdot n_i^*\cdot n_{k-1}^* \tag{16}$$

$\xi_{i,k-1}$ denotes a ratio of summaric volume of two colliding particles to the volume of a particle of class "'*k*".

## 4. Results of calculations

Simulation of agglomeration of alumina particles was based on equation (11). The vanishing of particles in a given group as a result of transition to a higher size level has been accounted for in the calculations. The behavior of $Al_2O_3$ particles was analyzed for a population of varying initial size 1, 3, 5, 10, 50 μm. The calculation of the population of particles produced in collisions is based on equations describing the frequency of collisions depending on the radius of particles and initial particles of a given radius quantity. The problem was presented in a simplified form; a small number of finite intervals of particle size were assumed (6 size groups). In real conditions the removal of 500 ppm of oxygen from steel generates about $6\cdot10^{14}$ alumina particles of radius 1μm in a volume of 1 m$^3$. The authors of this paper assumed the initial number of particles for about 30000. For all analyzed cases the process of turbulent collisions was simulated for given mixing energy values. L. Zhang [12] gives mixing energy values for the tundish conditions, which stay within the range of $5.3\cdot10^{-2}$ for entry zone, to $9.3\cdot10^{-5}$ for zone of non-turbulent flow. The rate of turbulent energy dispersion obtained by Nakaoka [7] in his water model ranged from 34.9 to 838 $10^{-4}$ m$^2\cdot$s$^{-3}$. The assumed mixing energy values 0.01 and 0.0001 m$^2\cdot$s$^{-3}$ stay within the interval of values for mixing energy in metallurgical

aggregates. The dimensionless time was defined each time from equations (15). This value stems from the number of particles taken into account when calculating mixing energy and agglomeration coefficient α. The values of coefficient α depend on the diameter of particles. In [8,13], α=0.3 was assumed for the diameter of particles equal to 1 μm, and α=0.03 for the diameter 70 μm. In [11] Higashini accounted for parameter α in the collision frequency equation (9) and defined it in experimental conditions from the following equations:

$$\propto = 0.727 \left[\frac{\mu r_1^3 (\varepsilon/v)^{1/2}}{A_{131}}\right]^{-0.242} \qquad (17)$$

where:
$A_{131}$ – Hamaker effective constant,
$\mu$ – viscosity of fluid [Pa·s],
$r_1$ – radius of basic particles [m],
For simulation purposes authors of this paper assumed $\alpha$=1 and used equation (7). Exemplary calculations for $Al_2O_3$ particles of radius 1, 3, 5, 10 and 50 μm are presented below. Six size groups were selected for presenting the density distribution of particular groups of particles. The plots of agglomeration plots of alumina particles for initial particles 1 μm, where the real time scale t was used for mixing energy: 0.01 and 0.0001 have been shown in Figs. 1-3.

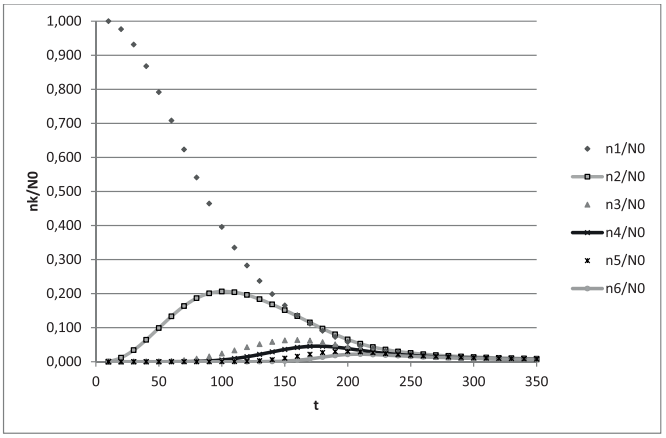


Fig. 1. Curves of particles vanishing due to agglomeration for initial size of inclusions 1μm at mixing energy 0.01 $m^2 \cdot s^{-3}$

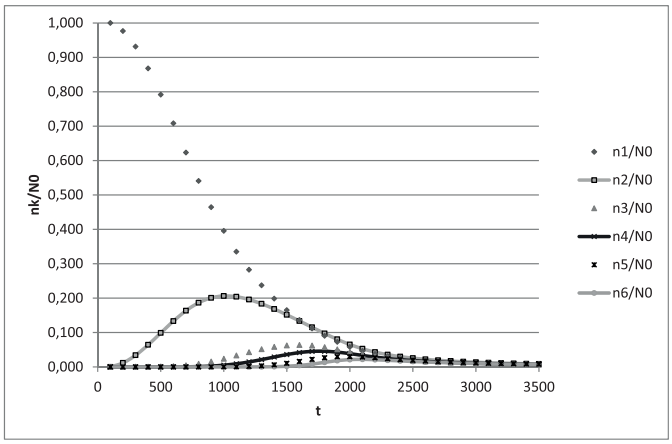


Fig. 2. Curves of particles vanishing due to agglomeration for initial size of inclusions 1μm at mixing energy 0.0001 $m^2 \cdot s^{-3}$

After 8 minutes, after intense mixing (ε=0.01 $m^2 \cdot s^{-3}$) there still remains a minimum population of particles of radius 1μm, which did not undergo agglomeration. Most of the particles already belong to group 6 of radius exceeding 3 μm. At low mixing energy (Fig. 2) the frequency of collisions between particles of initial radius 1 μm is hindered and requires longer time. In this case the agglomeration process lasts for about 80 minutes. In the case of very small particles, the process of their removal as a result of collisions is hindered. However they can be increased their size through diffusion processes. Figures 3-6 present curves of particles vanishing due to agglomeration for initial particles 3, 5 and 10 μm, where the real time scale *t* and the mixing energy: 0.01 and 0.0001 were used. In each case the time step had to be adjusted the curves for particular groups.

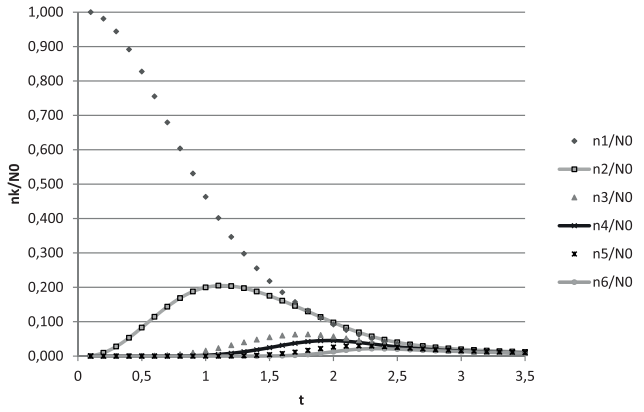


Fig. 3. Curves of particles vanishing due to agglomeration for initial size of inclusions 3μm at mixing energy 0.01 $m^2 \cdot s^{-3}$

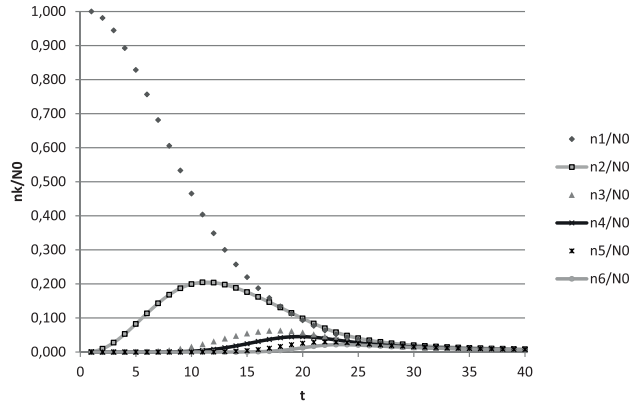


Fig. 4. Curves of particles vanishing due to agglomeration for initial size of inclusions 3μm at mixing energy 0.0001 $m^2 \cdot s^{-3}$

The character of the curves is analogous to the previous ones, though a rapid acceleration of the agglomeration process is observed with the increase of the radius of particles and the higher energies of mixing. Such a phenomenon was also observed in various works, e.g. Higashitani at al. [11]. The probability of collisions increases for particles of bigger radius as seen in figs. 3, 5 and 7. Figure 9 illustrates the influence of mixing energy on the agglomeration of particles of initial radius of 5μm, the time of agglomeration was presented in the logarithmic scale. When increasing the dynamics of mixing, the agglomeration process accelerates. The number of particles in group 1 started to decrease at constant rate from a certain

moment. The analysis of the influence of the mixing energy on the agglomeration reveals that the collision mechanism dominates in the case of bigger particles.

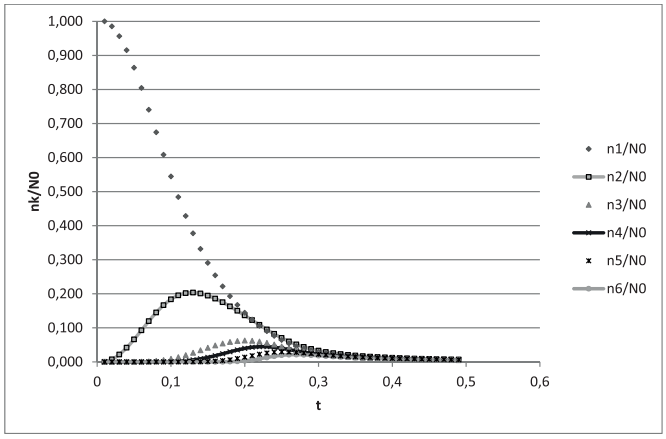


Fig. 5. Curves of particles vanishing due to agglomeration for initial size of inclusions 5μm at mixing energy 0.01 $m^2 \cdot s^{-3}$

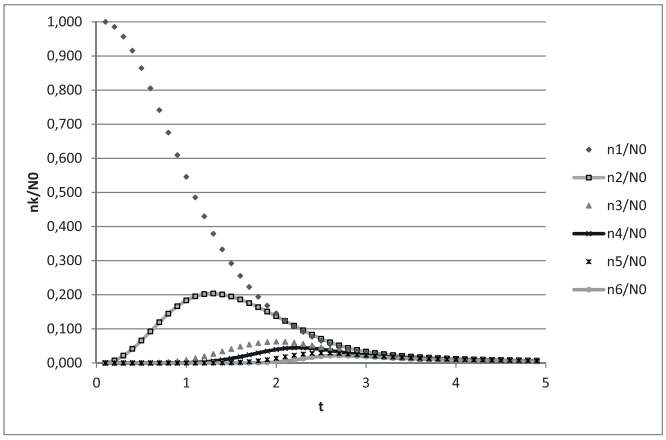


Fig. 6. Curves of vanishing particles due to agglomeration for initial size of inclusions 5μm at mixing energy 0.0001 $m^2 \cdot s^{-3}$

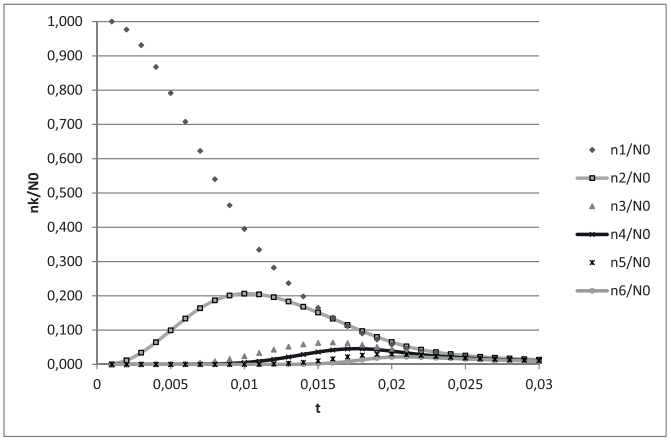


Fig. 7. Curves of particles vanishing due to agglomeration for initial size of inclusions 10μm at mixing energy 0.01 $m^2 \cdot s^{-3}$

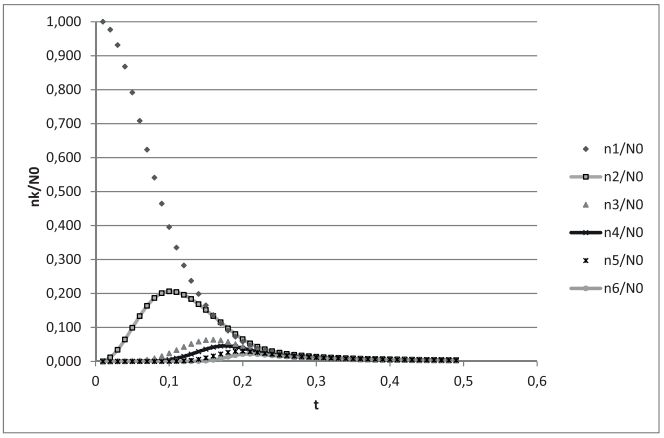


Fig. 8. Curves of particles vanishing due to agglomeration for initial size of inclusions 10μm at mixing energy 0.0001 $m^2 \cdot s^{-3}$

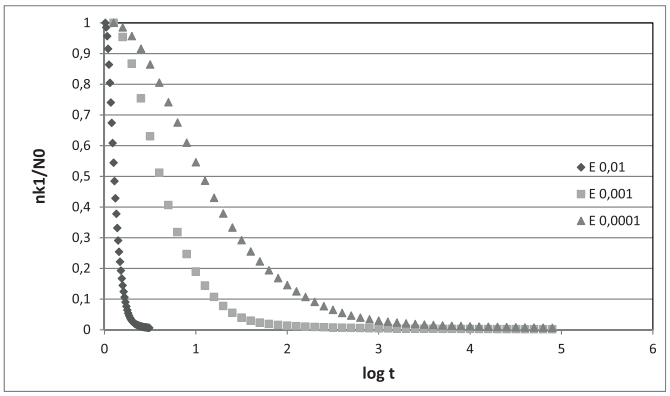


Fig. 9. Curves illustrating vanishing of particles in group 1 due to collision for initial particles of radius 5 μm

Figures 10 and 11 illustrate the influence of mixing energy on the agglomeration of particles of initial radius 50 μm.

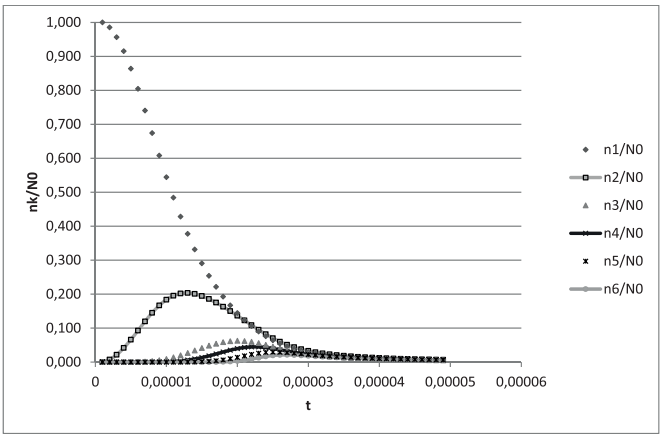


Fig. 10. Curves illustrating vanishing of particles due to agglomeration for initial size of inclusions 50μm at mixing energy 0.01 $m^2 \cdot s^{-3}$

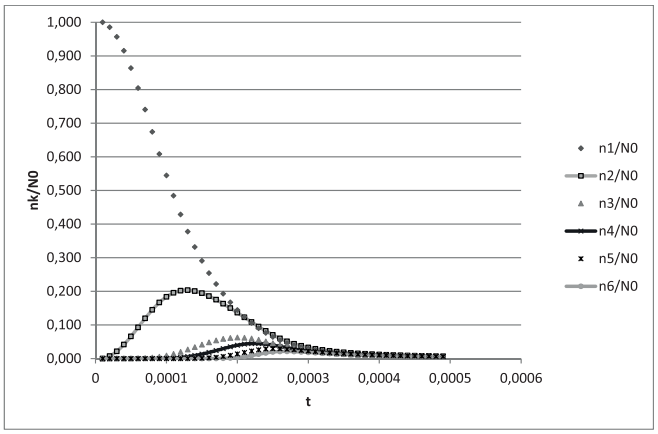


Fig. 11. Curves illustrating vanishing of particles due to agglomeration for initial size of inclusions 50μm at mixing energy 0.0001 $m^2 \cdot s^{-3}$

The analysis of influence of the energy of mixing on agglomeration reveals that the collision mechanism dominates in the case of bigger particles. In the real conditions the mixing of a metallic bath is non-homogeneous; at the bottom of the ladle the mixing is least efficient and the removal of inclusions, especially the small ones, may be difficult. As a result of collisions and due to whirls the particles change their volume, are removed as a result of operation of a few mechanisms simultaneously. Thus the increase and reduction of successive groups should be analyzed in view of these conditions. The course of the particle reduction curves in particular groups is congruent with the results of experiments and simulations, and the obtained results are analogous to the previous tests performed by many other authors [7,8,11]. As a result they do not give a complete picture of behavior of non-metallic inclusions in the process of steel refining and casting. The obtained results refer only to the agglomeration of particles caused by collisions, without taking into account for flotation and assimilation to slag.

## 5. Conclusions

The results of simulation show the dynamics of non-metallic inclusions removal in the bath as a result of turbulent collisions at a given energy of mixing. The applied calculation methodic accounts for the changing rate of mixing and initial size of the particles, for which the agglomeration process was investigated. The model takes into account the removal of a given group of particles through their collision with other members of this group, lower group or all higher groups. This task can be solved by solving the population balance equation. The calculation procedure does not account for other methods of particle removal, e.g. through flotation or assimilation to slag or refractory lining or flowing noble gas bubbles. It was established that the agglomeration process takes place much faster for bigger particles and at higher energy of mixing. In the case of bigger inclusions their agglomeration due to collisions takes place faster and this is caused by a higher probability that bigger particles will collide. The presented plots do not show the whole mechanism of particles removal but reveal the dynamics of the process. It was shown that after a given time there is always about 1% of particles left in each group. Their removal lasts much longer due to the considerable drop of probability of collision when the particles are less numerous. The presented results are aimed at showing differences in the agglomeration of inclusions through turbulent collisions. The applied procedure well illustrates the agglomeration of inclusions and can be used for modeling processes of steel refining.

**Acknowledgement**

This work was sponsored by Ministry of Science as the statute work – AGH UST - University of Science and Technology in Krakow (contract 11.11.170.318.14).

## REFERENCES

[1] H. Yin, H.Shibata, T. Emi, M. Suzuki, ISIJ Int. **37**, 946-955 (1997).
[2] H. Yin, H. Shibata, T. Emi, M. Suzuki, ISIJ Int. **37**, 936-945 (1997).
[3] T. Nakaoka, S. Taniguchi, K. Matsumoto, S. T. Johansen, ISIJ Int. **41**, 1103 – 1111 (2001).
[4] H. Lei, L. Wang, Z. Wu, J. Fan, ISIJ Int., **42**, 717-725 (2002).
[5] Q. Han, J. Hunt, ISIJ Int. **35**, 693 – 699 (1995).
[6] H. Shibata, Y. Hongbin, S. Yoshinaga, T. Emi, M. Suzuki, ISIJ Int. 38, 149-156 (1998).
[7] T. Nakaoka, S. Taniguchi, K. Matsumoto, S.T. Johansen, ISIJ Intern. **41**, 1103-1111 (2001).
[8] H. Tozawa, Y. Kato, K. Sorimachi, T. Nakanishi, ISIJ Int. **39**, 426 – 434 (1999).
[9] L. Zhang, B. Thomas 7th European Electric Steelmaking Conference, Venice, Italy, 26-29 May, 2.77-2.86 (2002).
[10] P. G. Saffman and J. S. Turner, On the Collision of Drops in Turbulent Clouds **1**, 16-30 (1956).
[11] K. Higashitani, K. Yamauchi, Y. Matsuno, G. Hosokawa, J. Chem. Eng. Jpn. **16**, 4, (1983).
[12] L. Zhang, S. Taniguchi, K. CaiMet. Materials Trans. B, **31B**, 253 – 266 (2000).
[13] J. Zhang, H. G. Lee, ISIJ Intern. **44** (2004).
[14] D. Kalisz, P.L. Żak, Acta Physica Polonica A **130**, 1, 157-159 (2016).
[15] P.L. Żak, D. Kalisz, J. Lelito, M. Szucki, B. Gracz, J.S. Suchy, Metalurgija **54**, 2, 357-360 (2015).